Journal of the Eastern Asia Society for Transportation Studies, Vol. 6, pp. 1368 - 1381, 2005

SOME FINDINGS OF CA MODEL TO GENERATE VARIOUS FREEWAY TRAFFIC FLOWS WITH ADDITIONAL RULES

Hyunho Chang
Traffic Specialist
Department of Traffic Management
Seoul Metropolitan Government
38 Seosomun Dong,
Jung gu, Seoul 100-110
South Korea
Fax:+82-2-723-0755
E-mail: nettrek@hanmail.net

SeungKirl Baek
Research Scientist
Transportation Research Group
Highway & Transportation Tech. Institute
Korea Highway Corporation
50-5, Sancheok-li, Dongtan-myeon
Hwasung-si, Gyeonggi-do 445-812
South Korea
Fax:+82-31-371-3319
E-mail: bsktrans@freeway.co.kr

Seong J. Namkoong
Senior Research Scientist
Transportation Research Group
Highway & Transportation Tech. Institute
Korea Highway Corporation
50-5, Sancheok-li, Dongtan-myeon
Hwasung-si, Gyeonggi-do 445-812
South Korea
Fax:+82-31-371-3319
E-mail: jake@freeway.co.kr

Byoungjo Yoon
Graduate Student
Department of Construction Transportation Engineering
Ajou University
231, Joongri Dong
Ichon-si, Gyeonggi-do 467-030
South Korea
Fax:+82-31-635-9194
E-mail: bjyoon63@hanmail.net

Abstract: It's reported that real traffic flow has three phases such as free, synchronized, and stop-and-go flow, and that macroscopic flow-density relationship, called the fundamental diagram, has various features such as inverted V-shaped, inverted U-shaped, bell-shaped, reversed λ-shaped, and reversed λ- shaped with upward concave. Cellular Automata (CA) theory for microscopic vehicle simulation modeling is capable of simulating large traffic road networks faster than real time using both memory-saved and high-computing data structure. Although simplified CA models are able to robustly reproduce the basic properties of uninterrupted traffic flow, they have shortcomings to the description of some flow-density relation diagrams such as revered λ- shaped with upward concave and bell-shaped relation. Based on existent CA Car-following models, this paper proposes an improved CA model integrating two additional rules for both stopping maneuver in the tail of traffic jam and low acceleration within traffic jam. Consequently, the improved CA model describes microscopic vehicle behaviors such as braking maneuver at the tail of traffic jam and low acceleration within congested traffic flow more realistic than present CA models and is able to reproduce various flow-density relationships including revered λ- shaped with upward concave and bell-shaped fundamental diagrams that existing CA models are hard to reproduce.

Key Words: Freeway Traffic Flows, Cellular Automata Model, Stopping Maneuver Rule, Low Acceleration Rule, Various Fundamental Diagrams.

1. INTRODUCTION

The modeling of traffic flow to describe traffic flow phenomena has more than half a hundred history from 1950s. Traditionally traffic flow model can be divided into macroscopic and

microscopic approaches. In macroscopic approaches, traffic flow is viewed as continuous and homogeneous particles akin to a fluid moving along a duct, and the basic philosophy of the macroscopic approach is the continuity equation that is based on densities and flows for a fluid-dynamical description. From pioneer to advanced fluid-dynamical traffic flow models have a hierarchical history; first order models, called the LWR model (Lighthill and Whitham, 1955; Newell, 1955; Richards 1956; Lax 1972; Daganzo, 1994, 1999), second order models (Payne, 1971, 1979; kerner and Konhauser, 1993; Daganzo, 1995; Papageorgiou et al, 1989; Michalopoulos et al, 1993; Zhang, 1998, 2000, 2002). In microscopic approaches, each vehicle is individually distinguished and treated with the so-called car-following theories. Generally three different car-following models have been prevailing; stimulus-response models, called the GM family of car-following models, based on the general idea that the response of a driver is a function of sensitivity and stimuli (Chandler et al, 1958; Gazis et al, 1959, 1961; May and Keller, 1967; Cedar and May, 1976; Ozaki, 1993), safe distance models using safe distance constraint to keep a certain spacing considering the velocities of the leader and the follower (Pipes, 1953; Kometani and Sasaki, 1958; Cheu et al, 1994; Newell, 2002), and collision avoidance models using collision avoidance constraint to determine the follower's acceleration rate, according to the velocity and position, to avoid back collision (Gipps, 1981).

These models have made great contributions to traffic flow modeling and simulation with their merits. But they propagate the traffic wave, namely density oscillation, in a deterministic way, and it is not straightforward to explain the stochastic features of such as stop-and-go motion, and the spontaneous formation of a jam, because they are developed from deterministic concept basically. In recent years, stochastic cellular automata models (CA) into the traffic flow modeling paved the way to describe the stochastic features by adding some random variables into a discrete time-and-space car-following concept. And especially CA models have allowed for the simulation of huge road networks faster than real time because of the advantage of a programming-oriented and computing memory-saved model structure (Beckman, 1997; Chopard, 1997; Schreckenberg, 2002).

However, CA models reproduce the basic features of traffic flows such as inverted V-shaped, inverted U-shaped, and reversed λ-shaped flow-density relationship but do not describe bell-shaped and reversed λ-shaped with upward concave fundamental diagrams, because simplified car-following, or movement, rules with not considering the velocity of the leader use "minimal information" on a spatial integer gap between the leader and the follower to update velocity. This deficiency of current CA models stems from the circumstances of early 1990s rudimental computer capability. As current state-of-the-art computing capability, it seems reasonable that more information about traffic flow conditions is used to the movement rules for the reproduction of more various features of traffic flows. Therefore, this paper employs two additional rules to tackle above problem, incorporates the two rules into (standard) NaSch model (**Na**gel and **Sch**reckenberg, 1992) soundly, and presents some different traffic flow features, through both trajectories of individual vehicles (according to time and space) and volume-density relations, that are reproduced with the developed CA model.

2. EXSTING STUDIES

2.1 Various Features of Traffic Flow

1) Some facts of traffic flows

The simplest empirical facts are the "spontaneous" formation of traffic jam, well known as the natural occurrence of phantom traffic jams. In the initial stage of the formation of spontaneous traffic jam, vehicles are very well separated individually and spatially. And a dense region appears without any reason such as car accidents, and road construction, and then leads to the formation of a jam that stays stable for certain duration but disappears again with no reason. During its lifetime, the head of the jam moves backwards against driving direction of the vehicles. One of the well-known phenomena in congested traffic is the "stop-and-go" phenomenon that occurs when disturbances are generated by the interference of low-speed vehicles. While the disturbances propagate backward, they strengthen or weaken. It seems reasonable that vehicles within each other state of congested flow change that lane for which the vehicle speed is higher. This lane-changing behavior increases the density of higher-speed lane and consequently decreases the vehicle speed. This process to balance the speed across lanes in dense enough traffic generates "synchronized" or "collective" traffic flow. Lots of experimental studies on stop-and-go and synchronized traffic have been reported as following. The density in stoppage wave is 60~87veh/km and the density following the stoppage wave is 39~53 veh/km, and the velocity of the wave is 14~17km/hr (Edie et al, 1967). The frequency of oscillation is 1/4 cycle a minute and the velocity of the back propagation is about 25kph (Mika et al. 1969). There exists a certain limit on the velocity fluctuation cycle, and the vehicle speed across different freeway lanes within the stop-and-go traffic can be changeable into synchronized traffic flow (Koshi et al, 1983). Real synchronized traffic flow has non-linear and dynamic properties and is distinguished as following (Kerner, 1996, 1997).

2) Various fundamental diagrams

The macroscopic features of traffic flow are usually described by three parameters: flow, density, and speed. The flow-density (q-k) relation, the so-called fundamental diagram, has a great deal of information about traffic flow, and has been revealed various relationships between flow and density. The early empirical studies have shown that the traditional q-k relations are parabolic curves and continuous (Greenshield, 1934; Greenberg, 1959). Some empirical research have revealed that there exists a gap, "the capacity drop", which means the fundamental diagram consists of two isolated curves and discontinuous; one curve with a positive slope for free flow and the other curve with a negative slope for congested traffic flow (Edie, 1958). The quantities of capacity drop are estimated about 5 to 6 percents (Hall et al, 1991), or 3 to 10 percents (Banks, 1991). The inverted-V type fundamental diagram is simple but effective (Atol, 1965). A study has postulated that an inverted-V type is one of appropriate choices (Hall et al, 1986), and that type is adopted in recent traffic flow studies, due to the simplicity and effectiveness (Daganzo, 1999; Newell, 1993). For an explanation of stop-and-go waves, a-mirror-image-of-the-Greek-letter-λ fundamental diagram, so-called reversed-λ type, has introduced which describes both free and congested traffic flows with the capacity drop with an important remark "In congested conditions drivers do not seriously follow the cars ahead as closely as they do in steady follow conditions, perhaps because they know that they are in oscillating flow and will be forced to decelerate again sooner or later. Because of this behavior drivers' average spacing are longer in congested conditions than in steady flow conditions" (Koshi et al, 1983). The reversed λ-shaped q-k relation is also explained and found with well-surveyed experimental data, and it has been found out that both the outflow, q_{out}, out of a wide jam and the maximal flow, $q_{\max}$, in free flow traffic approximately has the relation as $q_{\max} / q_{out} \approx 1.5$ (Kerner and Rehborn, 1996).

2.2 Particle Hopping Models

1) Discrete time and space models with a parallel computing

CA models are an artificial approach to simulation modeling based on movement rules to describe the intelligent decision-making behavior of automaton. Most of CA models are discrete in space and time, although a CA model uses continuous space and discrete time (Krauss et al, 1997). In the present paper we focus on one-dimensional, namely single-lane, CA models using a discrete time-and-space dimension. About decade years ago, the NaSch model, a stochastic CA model for single-lane freeway traffic, has been launched into the world (**Na**gel and **Sch**reckenberg, 1992). In a CA, a road system, divided by constant length is composed of lattices. Individual cell can either be empty or occupied by exactly one car. At time t, the emptiness of a cell is depicted by integer value –1, and the occupation of a cell, the state of vehicle is characterized by occupying vehicle's velocity (cell/sec), integer values $v_i(t) = \{0,1,...,v_{\max}\}$, that is also discrete due to discrete in time and space. For a simple description of freeway traffic, the length of each lattice is about 7.5m, the space occupied by a car in a jam density including bumper-to-bumper space. And time step for velocity updating is 1.0 sec that is the shortest reaction time of drivers in real time. NaSch model is in parallel computing with noise mechanism, and is composed of following three steps:

- Step 1: Deterministic velocity updating: $v_i(t+1) = \min\{g_i,\ v_i(t)+1,\ v_{\max}\}$
- Step 2: Randomization with p_{noise}: if (random value $< p_{noise}$) then
  $v_i(t+1) = \max\{v_i(t+1)-1,\ 0\}$
- Step 3: Movement with updated velocity: $x_i(t+1) = x_i(t) + v_i(t+1)$

Here g_i denotes the gap, the number of unoccupied cells from the follower (i) to the leader ($i+1$) at time (t), and p_{noise} is noise parameter (0.0~1.0).

The NaSch model is a minimal model in the sense that it reproduces the basic features of real traffic using minimal information about both the state of particle and the gap for updating velocity. With the use of a parallel computing that consider the reaction time and lead to a series of overreaction, the NaSch model with noise parameter generates, when $p_{noise} > 0.0$, the formation of spontaneous jams that reproduce inverted U-shaped fundamental diagrams, and when $p_{noise} = 0.0$, the CA model is called as the deterministic CA, describes inverted V-shaped fundamental diagrams. Some experiment studies suggest that the capacity drop in the reversed λ-shaped fundamental diagram takes a key role in the occurrence of meta-stable states with long lifetimes (Koshi, 1983; Kerner and Rehborn, 1996). The NaSch model doesn't describe meta-stable state and hysteresis. However, The NaSch model with the slow-to-start (s2s) rule, called the Velocity-Dependent-Randomization (VDR) model in which the randomization parameter depends on the velocity of the car, reproduces a reversed λ-shaped fundamental diagram. The VDR model uses random noise parameter (p_s), higher value than p_{noise}, to depict the low acceleration of stopped vehicles. If $p_s >> p_{noise}$ ($\forall\, v_i(t) = 0$), $p_s = p_{noise}$ ($\forall\, v_i(t) > 0$) then, drivers escaping out of a jam will hesitates so that the jam grows and moves backward. And if $p_s = p_{noise}$ ($\forall\, v_i(t)$) then, the VDR model has the same function as the NaSch model (Barlovic et al, 1998). The s2s rule is introduced in the T^2 model (Takayasu and Takayasu, 1993). In the update rules of T^2 model like those of the NaSch model, stopped vehicles with only one empty cell in front of them accelerate with probability $(1-p_t)$, whereas the other vehicles increase their speed deterministically. When

$v_{\max}$ is higher than 1, T^2 model also reproduces a reversed λ-shaped fundamental diagram (Barlovic et al, 1998).

2) Shortcomings of present CA models

Figure 1 illustrates from convex-shaped to reversed λ-shaped with upward concave fundament diagrams. In discrete CA models, a range of densities $\rho_0 < \rho < \rho_1$ is consist of velocity $\{v_{\max}, v_{\max} - 1\}$ and $\rho_4 < \rho < \rho_5$ is be made up of velocity $\{0,1\}$, which the homogeneous traffic flow is linearly stable against any disturbance, whereas there is an density interval $\rho_2 < \rho < \rho_3$ where homogeneous traffic is linearly instable, which means that homogeneous traffic flow collapse into heterogeneous traffic like stop-and-go traffic by a disturbance. There are regions defined by ρ_1 and ρ_4 ($\rho_1 < \rho < \rho_2$ and $\rho_3 < \rho < \rho_4$) where CA models are meta-stable, which means the homogeneous and the heterogeneous traffic respectively exist stable. Especially, in density regimes $\rho_1 < \rho < \rho_2$ the fundamental diagram can consist of two branches, a homogeneous and a heterogeneous state. In the upper regime, there is a jam-free state, and in the lower regime, the traffic flow system is in a phase-separated state that consists of a (wide) jam and a free-flow traffic. So CA models have to respectively explain the two regimes, bounded by ρ_2 and ρ_5 (i.e. $\rho_2 < \rho < \rho_3$ and $\rho_4 < \rho < \rho_5$), to reproduce more various q-k relations.

Aforementioned one-dimensional CA models microscopically have the two weaknesses. The one is the high braking capability that comes from the deterministic velocity-updating rule. When $v_i(t) < g_i$, $v_i(t+1)$ is updated as $v_i(t+1) = g_i$ by $\min\{g_i, v_i(t)+1, v_{\max}\}$, which results in the unrealistic braking to avoid back collision in one time step, generally 1 second, from $v_{\max}$ to 0. The other is high acceleration within a (wide) jam, which is related to the limitations of the role of noise parameters that do not distinguish drivers' accelerating behaviors between staying within a jam and escaping out of it. Therefore the discrete CA models using minimal information, namely the gap, have defects to reproduce more various fundamental diagrams, because of the limitation to describe the concave-shaped q-k relationship in congested traffic flow regimes.

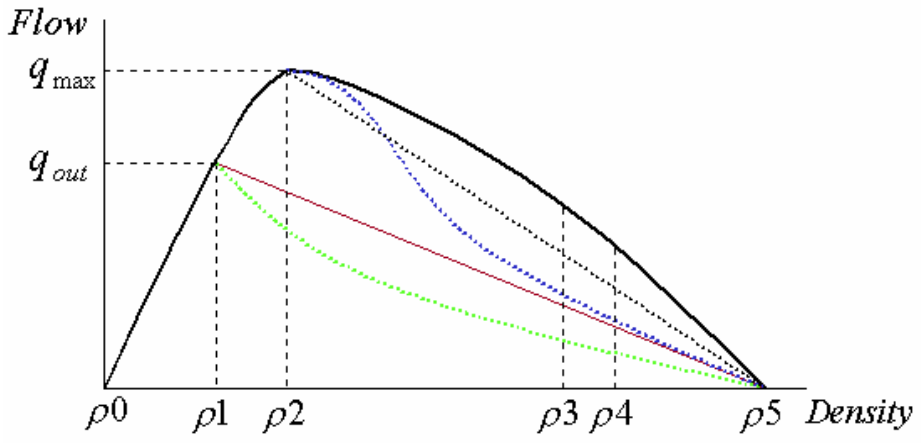

Figure 1. Stylized fundamental diagram: ρ_i respectively means the various points of instability, and $q_{\max}$ maximal flow in homogeneous and free flow traffic, q_{out} the outflow out of a (wide) jam in reversed λ types.

3. DEVELOPMENT OF AN UPDATED CA MODEL WITH ADDITIONAL RULES

3.1 Additional Rules For More Realistic Behaviors

In this paper, two additional rules, **S**topping **M**aneuver **R**ule (**SMR**) and **L**ow **A**cceleration **R**ule (**LAR**), is introduced to tackle aforementioned two defects and to capture velocity quantities more realistically under the heterogeneous traffic flow conditions. SMR is to describe the braking of a running vehicle following a stopped vehicle. LAR is to capture the low accelerating behavior of a stopped vehicle tailgating a stopped vehicle. And then the two rules are integrated into the (standard) NaSch model with s2s rule, called the VDR model.

An approaching vehicle with velocity ($v_i(t) > 0$, cell/sec) to the back of a stopped leading vehicle whether keeps its velocity but not accelerating if there is enough distance between it and the stopped leading vehicle, or can not help slowing down to protect itself from a rear-end collision or a crash if it has distance not enough to keep its velocity. This decelerating process is determined by both not-accelerating distance (d_o) and start-braking distance (d_b) that is given by

$$d_o = \sum_{i=1}^{k} i \quad k = \min\{v_i(t)+1, v_{\max}\}, \text{ for all vehicles with } \; v_i(t) > 0$$

$$d_b = \sum_{i=1}^{k} i \quad k = v_i(t), \text{ for all vehicles with } \; v_i(t) > 0$$

And then with d_s, the number of unoccupied cells from vehicle (i) to the first stopped vehicle at time (t), the stopping manoeuvre can be described: if $d_o \geq d_s > d_b$ then a vehicle will be apt to keep its velocity without acceleration, and if $d_b \geq d_s$ then a vehicle have to decelerate its velocity through braking maneuver process. With noise parameter (p_{sm}, $p_{noise} \leq p_{sm} \leq 1.0$) that is higher value than 0.9 because the stopping process is inevitable, SMR is given:

-Step 0: Determination of the randomization noise parameter

if $d_b \geq d_s$ and $v_i(t) \leq g_i$ then $p_n = p_{sm}$

else $p_n = p_{noise}$

-Step 1: Deterministic velocity updating

if $d_o \geq d_s$ then $v_i(t+1) = \min\{g_i, v_i(t), v_{\max}\}$

else $v_i(t+1) = \min\{g_i, v_i(t)+1, v_{\max}\}$

-Step 2, 3: following those of the NaSch model

In the VDR model, one of the two noise parameters, namely p_s, is applied for the acceleration of both stopped vehicles within a wide (moving) jam and escaping vehicle from it with the same noise value. But an accelerating maneuver with high acceleration rate to escape a jam is different from a low accelerating maneuver within a heavy jam. Because, in a heavy traffic jam, the accelerating maneuver is physically accomplished with low acceleration rate and drivers psychologically hesitate to accelerate. To describe this low-accelerating behavior within a wide-moving jam, LAR is introduced. Let us make assumption: A stopped

vehicle ($v_i(t)$) with g_i=1 following a stopped vehicle ($v_{i+1}(t)$) at time (t) stays within a jam, whereas a sopped vehicle ($v_i(t)$) with g_i=1 following a running vehicle ($v_{i+1}(t)$) at time (t) escapes out of it. In LAR, noise parameter (p_{la}, $p_s \le p_{la} \le 1.0$) is higher value than p_s so that a stopped vehicle following a stopped vehicle will accelerate with probability $1-p_{la}$. LAR is given by:

-Step 0: Determination of the randomization noise parameter

if $v_i(t)=0$ then

if $g_i=1$ and ($v_{i+1}(t)=0$ or $g_{i+1}=0$) then $p_n = p_{la}$

else $p_n = p_s$

Here g_{i+1} is the gap of the vehicle $(i+1)$ in front of the vehicle (i) at time (t)

-Step 1, 2 and 3: following those of the NaSch model

SMR and LAR are directly and easily integrated with the VDR model with step 0, the determination of the randomization noise parameter as following:

-Step 0: Determination of the randomization noise parameter

$p_n = p_{noise}$

if $v_i(t)=0$ then

if $g_i=1$ and ($v_{i+1}(t)=0$ or $g_{i+1}=0$) then $p_n = p_{la}$

else $p_n = p_s$

if $v_i(t)>0$ then

if $d_b \ge d_s$ and $v_i(t) \le g_i$ then $p_n = p_{sm}$

else $p_n = p_{noise}$

-Step 1: Deterministic velocity updating

if $d_o \ge d_s$ then $v_i(t+1) = \min\{g_i,\ v_i(t),\ v_{\max}\}$

else $v_i(t+1) = \min\{g_i,\ v_i(t)+1,\ v_{\max}\}$

- Step 2: Randomization with p_n:

if (random value $< p_{noise}$) then $v_i(t+1) = \max\{v_i(t+1)-1,\ 0\}$

- Step 3: Movement with updated velocity: $x_i(t+1) = x_i(t)+v_i(t+1)$

The developed CA model based on the VDR model with SMR and LAR has convertibility and describes multi-regime fundamental diagrams (hereafter let us to call this CA model as a Multi-Regime-Oriented (MRO) model). If $p_{noise} = p_s = p_{sm} = p_{la}$ and $p_{noise} < 0.5$ then the MRO model has the same function as the (Standard) NaSch model, and if $p_{noise} << p_s$, $p_{noise} = p_{sm}$, $p_s = p_{la}$ then as the VDR model. The homogeneous traffic ($\rho_0 < \rho < \rho_2$), see Fig. 1, consisting of velocity $\{v_{\max}, v_{\max}-1\}$ is captured by p_{noise} that give linearly stable solutions, the free-flow velocity $v_f = v_{\max} - p_{noise}$ therefore the homogeneous flow $J_{\hom}(\rho) = \rho(v_{\max} - p_{noise})$, where $\rho = k / k_{jam}$. In the VDR model the flow in the phase-separated regime ($\rho_1 < \rho < \rho_5$) is given by $J_{sep}(\rho) = (1-p_s)(1-\rho)$ (Barlovic et al, 1998). If $p_{la} > p_s$ then the stable states ($\rho_4 < \rho < \rho_5$) is described by p_{la}, and if $p_{sm} > p_{noise}$ then

the instable states ($\rho_2 < \rho < \rho_3$) is explained by the combination of p_{noise} and p_{sm}.

3.2 Versatility of the Developed Model

The MRO model reproduces various fundamental diagrams according to how to combine the noise parameters. To show the variety, the combination scenarios of noise parameter are introduced in Table 1. On the one hand scenario 1 has same function as the NaSch model and scenario 3 has the capability to reproduce the fundamental diagram described with the VDR model, but on the other scenario 2 and 4 are respectively the form of the NaSch model and the VDR model that are including SMR and LAR.

Table 1. The combination scenario of noise parameters

Scenario	p_{noise}	p_s	p_{sm}	p_{la}
1	$p_{noise} = p_s$		$p_{noise} = p_{sm}$	$p_{noise} = p_{la}$
2			$p_{noise} < p_{sm}$	$p_{noise} < p_{la}$
3	$p_{noise} < p_s$		$p_{noise} = p_{sm}$	$p_s = p_{la}$
4			$p_{noise} < p_{sm}$	$p_s < p_{la}$

Inverted V-shaped fundamental diagram is described by scenario 1 with $p_{noise} = 0.0$. If $p_{noise} = 0.0$, the MRO model gives linear solutions like deterministic CA model in both free and congested flow state. Figure 2 and 4 shows the vehicle trajectories of scenario 1, 2, 3, and 4 respectively, where traffic jams are generated spontaneously and grows or decays going back to the upstream when spontaneous perturbations give rise to traffic jams at higher densities.

The space-time trajectories of scenario 1 and 3 describe the braking of vehicles following stopped vehicles all on the sudden and with unreality because of the shortcomings of the NaSch model's deterministic velocity updating rule to the description of stopping maneuver, whereas the vehicle trajectories of scenario 2 and 4 using SMR well depicts braking maneuver with more realistic deceleration process than those of scenario 1 and 3. In space-time diagrams of scenario 1 and 3 the average velocity within traffic jam is very low and especially the velocities of vehicles within a jam are almost 0, namely locked-up, in scenario 3, because an approaching vehicle to the tail of jam arrives to the rear end of a stopped vehicle with too high unrealistic braking capability and an vehicle within jam too aggressively speeds up with p_{noise} or p_s. So the traffic phase in congested traffic is divided into free flow and heavily jammed flow. In space-time trajectories of scenario 2 and 4 the average velocity within traffic jam is rather higher than that of scenario 1 and 3, because an approaching vehicle to the tail of jam arrives with more or less one cell between it and a front stopped vehicle using SMR and an stopped vehicle with one gap lagging a stopped vehicle described by LAR has lower acceleration capability than that of scenario 1 and 3, which mean a vehicle reaches to the tail of jam and then it experiences low speed and stopping within jam. So the density of a jam is lower and the length of it is wider, and the shock wave speed of it is higher than scenario 1 and 3.

Above differences of microscopic behavior consequently generate various fundamental diagrams illustrated in Figure 3 and 4. On the one hand Scenario 1 reproduces an inverted U-

shaped fundamental diagram that explains flow-density relationships in congested flow states like a convex relation, but on the other hand scenario 2 with SMR and LAR reproduces bell-shaped fundamental diagram that depicts flow-density relationship like concave shape.

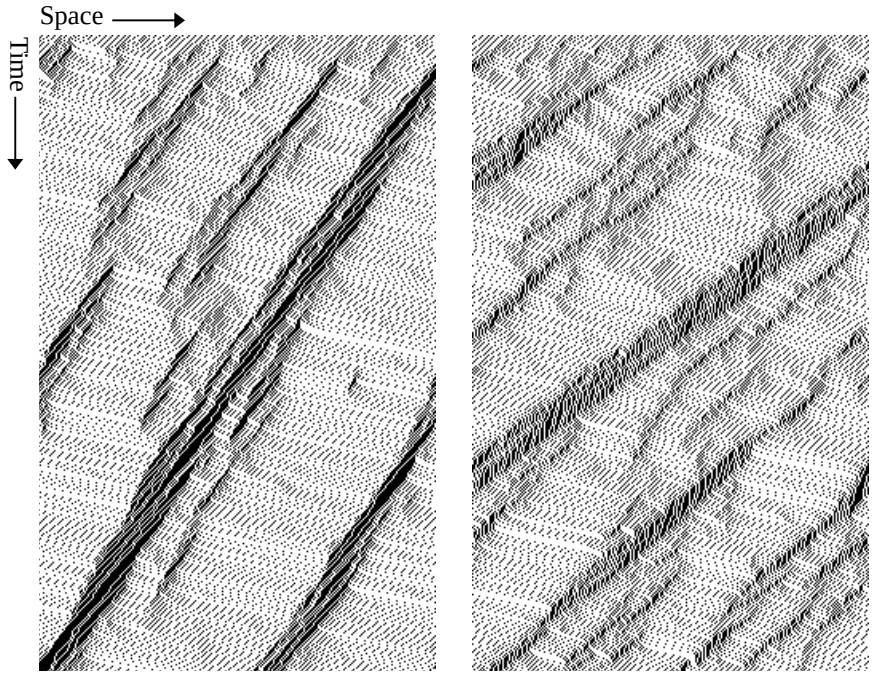

Figure 2. Vehicle trajectories on one-lane periodic system with parallel update: dots represent vehicles that move toward right according to the time direction to the down. Flow state is homogeneous at time step = 0. System size: $v_{\max} = 5$ cells/sec, cell length = 7.5m, $\rho = 0.25$ (≈ 33 Vehicles/km). Left: scenario 1 ($p_{noise} = 0.135$). Right: scenario 2 ($p_{noise} = 0.135$, $p_{sm} = 0.95$, $p_{la} = 0.75$).

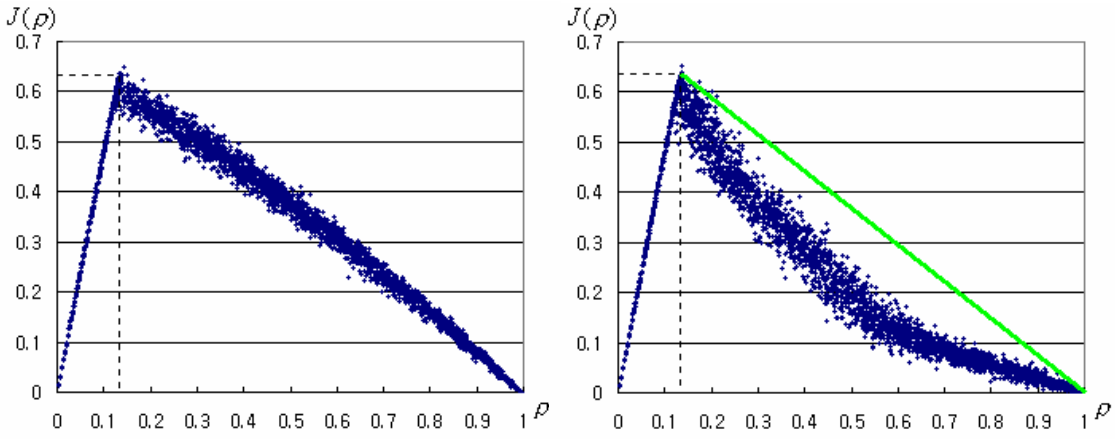

Figure 3. Fundamental diagrams of scenario 1 and 2: 5-min polling average flow-density. System size: 10 km $\approx 1{,}333$ (=10,000/7.5) cells, $v_{\max} = 5$ cells/sec, cell length = 7.5m. Left: scenario 1 ($p_{noise} = 0.135$). Right: scenario 2 ($p_{noise} = 0.135$, $p_{sm} = 0.95$, $p_{la} = 0.75$). Flow $J(\rho)$ is given by $\rho \times s(\rho)$, where $s(\rho)$ is velocity at density $\rho = k / k_{jam}$, therefore q (vehicle/hour) is considered by $J(\rho) \times 3{,}600$.

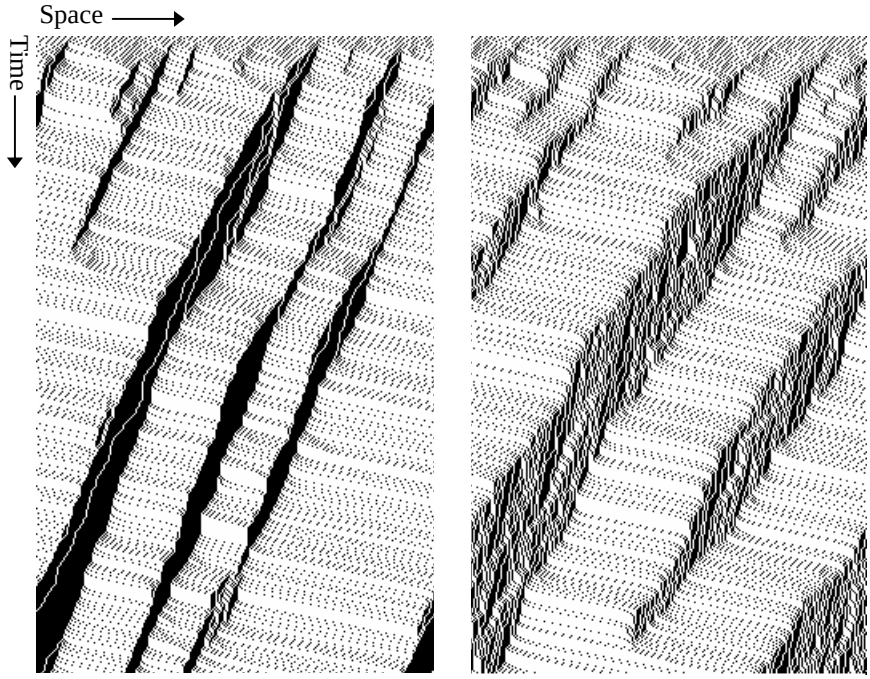

Figure 4. Vehicle trajectories on a ring system with parallel update: the initial flow state and the system size comply with Fig. 2. Left: scenario 3 ($p_{noise} = 0.135, p_s = 0.5$). Right: scenario 4 ($p_{noise} = 0.135, p_s = 0.5, \ p_{sm} = 0.95, \ p_{la} = 0.75$).

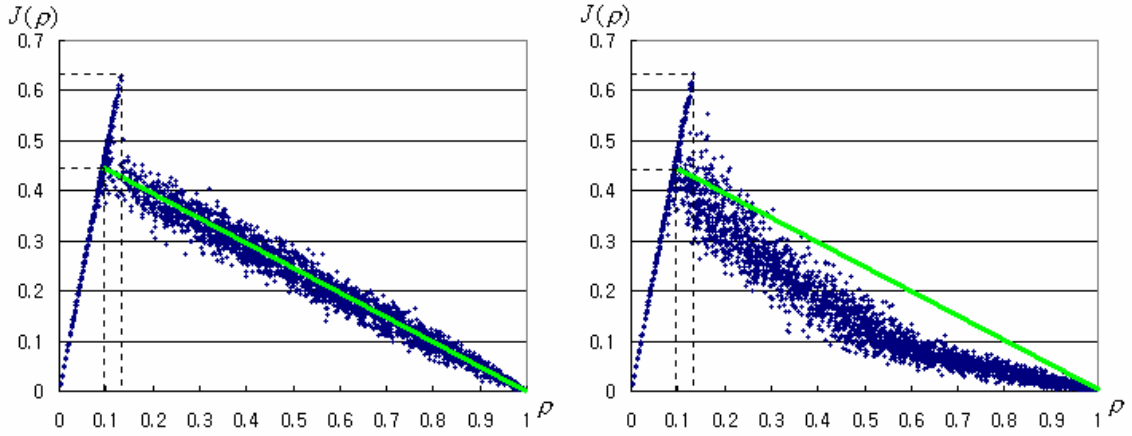

Figure 5. Fundamental diagrams of scenario 3 and 4: 5-min polling average flow-density. The system size complies with Fig. 3. Left: scenario 3 ($p_{noise} = 0.135, p_s = 0.5$). Right: scenario 4 ($p_{noise} = 0.135, p_s = 0.5, \ p_{sm} = 0.95, \ p_{la} = 0.75$).

While the flows escaping out of jams is explained by p_{noise} in Figure 2, those is captured by p_s in Figure 4, which means if $p_s >> p_{noise}$ and inflow arriving to the tail of a jam is higher than or equal to outflow escaping from it, a jam will continues to grow backward and not to decay. Consequently this traffic flow behavior generates reversed λ-shaped fundamental diagrams illustrated in Figure 5. Scenario 3 reproduces reversed λ-shaped q-k relationship that in congested flow state shows straight q-k relation, which means traffic flow state is

totally explained with a heavily-jammed state and a homogeneous free flow state, whereas scenario 4 describes reversed λ-shaped fundamental diagram with upward curve that in congested flow state is explained with upward concave q-k relation, which reproduces traffic flow state is described with a homogeneous free flow regime and a jammed state, but not lock-up. In meta-stable state, the fundamental diagrams are composed of two branches, where in the upper regime with positive slope there is no acting upon each other vehicles and the flow state stays homogeneous and free-flow. However, in the lower regime with negative slope the flow state is phase-separated and consists of large jams and free flows.

The simulation performs on a contemporary desktop (Pentium3, CPU 640 MHZ, SD RAM 128 MB, HDD 20 GB), and one-hour simulation takes 1,033 seconds, about 3.5 times faster than real time, to simulate 885,115 ($= \sum_{i=1}^{1,333} i$) vehicles in a large system (13,330 lane-km). Notwithstanding the computational power of state-of-the-art computers and steeply growing computer technology, it leaves the application of the MRO model to the simulation modeling of a large freeway network.

4. CONCLUSIONS

In this research, to address both braking behavior arriving to the tail of traffic jam and low acceleration within it and to prevent lock-up phenomenon, SMR (Stopping Maneuver Rule) and LAR (Low Acceleration Rule) are introduced and integrated into the NaSch model with s2s rule, called the VDR model. SMR successively explains the mandatory deceleration or braking behavior of arriving vehicles to the tail of traffic jam, and LAR effectively depicts the low acceleration behavior within traffic jam. And the updated CA model with additional rules, SMR and LAR, is simulated in the one-lane circuit system with a combination scenario of random noise for s2s, SMR, and LAR rule.
In result, microscopically the two rules robustly depict vehicle's speed at the tail of and within jam more realistically than the other discrete time-space CA models, and can prevent lock-up conditions within jam. Macroscopically, the performance of the MRO model macroscopically describes vehicle behaviors more realistically than the discrete time and space CA models. And the presented model reproduces basic fundamental diagrams such as, inverted V-shaped, inverted U-shaped, and bell-shaped, and generates currently indicated q-k relationships such as reversed λ-shaped, and reversed λ- shaped with upward concave with high computing speed faster than real time.

REFERENCES

1) Books and Books chapters

Payne H. J. (1979). A critical review of macroscopic freeway model. In W. S. Levine (ed.), **Research Directions in Computer Control of Urban Traffic Systems**, 251-265. American Society of Civil Engineers, New York

2) Journal papers

Atol P. J. (1965) Interdependence of certain operational characteristics within a moving traffic stream. **Highway Research Record 72**, 58-57

Banks J. H. (1991) Two-capacity phenomenon at freeway bottleneck: A basis for ramp metering? **TRR 1320**, 83-90

Barlovic R., Santen L., Schadschneider A., and Schreckenberg M. (1998) Metastable states in CA models for traffic flow. **European Physical Journal B, Vol. 5**:793

Chandler R. E., Herman R., and Montroll W. (1958) Traffic dynamics: studies in car-following. **Operation Research 6**, 165-184

Cedar A., and May A. D. (1976) Further evaluation of single and two regime traffic flow models. **TRR 567**, 1-30

Cheu R. L., Recker W. W., and Ritchie S. G. (1994) Calibration of INTRAS for simulation of 30-sec loop detector output. **TRR 1457**, 208-215

Daganzo C. F. (1994) The cell transmission model: a simple dynamic representation of highway traffic. **Transpn. Res. B, Vol. 28**, 269

Daganzo C. F. (1995) Requiem for second-order fluid approximations of traffic flow. **Transpn. Res. B, Vol. 29**, 277-286

Gazis D. C., Herman R., and Potts R. B. (1959) Car-following theory of steady-state traffic flow. **Operation Research 7**, 499-505

Gazis D. C., Herman R., and Rothery R. W. (1961) Nonlinear following-the-leader models of traffic flow. **Operation Research 9**, 545-565

Gipps P. G. (1981) A behavioral car-following model for computer simulation. **Transpn. Res. B, Vol. 15**, 105-111

Hall F. L., Allen B. L., and Gunter M. A. (1986) Empirical analysis of freeway flow-density relationships. **Transpn. Res. A, Vol. 20**, 197-210

Hall F. L., and Agyemang-Duah K. (1991) Freeway capacity drop and the definition of capacity. **TRR 1320**, 91-98

Kerner B. S. and Rehborn H. (1996) Experimental features and characteristics of traffic jams. **Physical Review E, Vol. 53**, R1297-R1300

Kerner B. S. (1998) Experimental features of self-organization in traffic flow. **Physical Review Letters, Vol. 81**, 3739-3800

Kometani E., and Sasaki T. (1958) On the stability of traffic flow. **Journal of the Operations Research Society of Japan**, 11-26

May A. D., and Keller H. E. M. (1967) Non integer car-following models. **Highway Research Record 199**, 19-32

Michalopoulos P. G., Yi P., and Lyrintzis A. S. (1993) Continuum modeling of traffic

dynamics for congested freeways. **Transpn. Res. B, Vol. 27**, 315-332

Mika H. S., and Kreer J. B., and Yuan L. S. (1969) Dual mode behavior of freeway traffic. **Highway Research Record 279**, 1-12

Nagel K., and Schreckenberg M. (1992) A Cellular automaton model for freeway traffic. **Journal of Physics I France, Vol. 2**, 2221-2229

Newell G. F. (1955) Mathematical models of freely moving traffic. **Journal of the Operations Research Society of America, Vol. 3**, 176-188

Newell G. F. (2002) A simplified car-following theory: a low order model. **Transpn. Res. B, Vol. 36**, 195-205

Papageorgiou M., Blosseville J. M. and Haj-Salem H. (1989) Macroscopic modeling of traffic flow on the Boulevard Peripherique in Paris. **Transpn. Res. B, Vol. 23**, 29-47

Pipes L. A. (1953) An operational analysis of traffic dynamics. **Journal of Applied Physics, Vol. 24**, 274-287

Richards P. I. (1956) Shockwaves on the highway. **Operation Research 4**, 42-51

Takayasu M., and Takayasu H. (1993) Phase transition and 1/f type noise in one dimensional asymmetric particle dynamics. **Fractals, Vol. 1**, 860-866

Zhang H. M., and Kim T. (2000) Effects of relaxation and anticipation on Rieman solutions of Payne-Whitham model. **TRR 1710**, 131-135

Zhang H. M. (1988) A theory of nonequilibrium traffic flow. **Transpn. Res. B, Vol. 32**, 485-498

Zhang H. M. (2002) A non-equilibrium traffic model devoid of gas-like behavior. **Transpn. Res. B, Vol. 36**, 275-290

3) Papers presented to conferences

Chopard B., Dupuis A., and Luthi P. (1997) A Cellular Automaton model for Urban Traffic and its Application to the City of Geneva. **Traffic and Granular Flow '97**, Springer, 153-168

Edie L. C., and Baverez E. (1967) Generation and propagation of stop-and-start traffic waves. **Vehicular Traffic Science, Proceedings of the 3rd Intl. Symp**. **On the Theory of Traffic Flow**, New York, 26-37

Edie L. C., and Foote R. S. (1958) Traffic flow in tunnels. **Highway Research Board Proc**. 37, 66-67

Kerner B. S. (1997) Traffic Flow: Experiment and Theory. **Traffic and Granular Flow '97**, Springer, 239-267

Koshi M., Iwasaki M., and Ohkura I. (1983) Some findings and an overview on vehicular

flow characteristics. **Proceedings of the 8th Intl. Symp. On Transportation and Traffic Flow Theory**, Hurdle V., Hauer E., Stuart G. (eds.), 403-426

Krauss S. (1997) Microscopic Traffic Simulation: Robustness of a Simple Approach. **Traffic and Granular Flow '97**, Springer, 269-283

Lighthill M. J., and Whitham J. B. (1955) On kinematic waves. I: Flow movement in long rivers. II: A Theory of traffic flow on long crowded roads. **Proceedings of the Royal Society A, Vol. 229**, 317-345

Ozaki H. (1993) Reaction and anticipation in the car-following behavior. **Proceedings of the 13th Intl. Symp. On Transportation and Traffic Theory**, 349-366

Payne H. J. (1971) Models of freeway traffic and control. **Simulation Councils Proc. Series: Mathematical Models of Public Systems, Vol. 1**, G. A. Bekey (ed.), 51-61

Schreckenberg M. et al, (2002) Simulation of the Autobahn in North Rhine-Westphalia. **Proceedings of the International Symposium on Transport Simulation**, Kitamura R., and Kuwakara M. (eds.), 193-199

4) Other documents

Beckman R. J. et al, (1997). TRANSIMS Dallas/Fort Worth case study report. Los Alamos Unclassified Report LA-UR to be released, Los Alamos National Laboratory, TSA-Division, Los Alamos NM 87545, USA

Daganzo C. F. (1999). A behavioral theory of multi-lane traffic flow. I: Long homogeneous freeway sections. Technical Report Research Report UCB-IST-RR-99-6, Institute of Transportation Studies, University of California at Berkeley

Lax P. D. (1972). Hyperbolic systems of conservations laws and the mathematical theory of shock waves. Society for Industrial and Applied Mathematics, Philadelphia, PA